Astron. Astrophys. 352, 248–256 (1999)

ASTRONOMY AND ASTROPHYSICS

ASCA X-ray observations of the super-metal-rich stars 30 Ari and η Boo

A. Maggio[1], **F. Favata**[2], **H. Negoro**[3], **N.S. Brickhouse**[4], **and A.K. Dupree**[4]

[1] Osservatorio Astronomico di Palermo "G.S. Vaiana", Palazzo dei Normanni, 90134 Palermo, Italy
[2] Astrophysics Division – Space Science Department of ESA, ESTEC, Postbus 299, 2200 AG Noordwijk, The Netherlands
[3] Institute of Physical and Chemical Research (RIKEN), 2-1 Hirosawa, Wako, Saitama, 351-0198, Japan
[4] Smithsonian Astrophysical Observatory, 60 Garden Str., Cambridge, MA 02138, USA

Received 9 June 1999 / Accepted 8 September 1999

Abstract. We present X-ray observations of two late-type stars, HR 764 (30 Ari B, F4V) and HR 5235 (η Boo, G0IV), with photospheric metal abundances about twice the solar value. We have derived the coronal temperatures and metallicities of these stars, and compared them with those of other stellar X-ray sources with solar or sub-solar photospheric composition, already observed with ROSAT and ASCA. The X-ray spectra of the two targets can be fitted with isothermal models yielding temperatures of 6.2 MK and 3.5 MK, and X-ray luminosities $\log L_{\rm x}$ = 29.6 and 28.1 erg s^{-1}, for HR 764 and HR 5235 respectively. The best-fit model for HR 764, including a gaussian component which accounts for Fe XVII line emission from highly excited states, yields for its corona a solar (photospheric) iron abundance, while the best-fit iron abundance for HR 5235 is about half solar; however, in both cases, the uncertainties do not allow excluding values consistent with photospheric metallicities. Instead, the data indicate significant overabundances of Mg and Si by factors 2–3 with respect to the Fe abundance, and suggest low $\rm O/Fe$ abundance ratios. We conclude that these two super-metal-rich stars appear to have coronal properties similar to those of other F and G main-sequence stars with "normal" photospheric abundances: in particular, HR 764 looks similar to the Hyades F stars, while the coronal temperature, luminosity and abundances of HR 5235 are similar to those of other field G dwarfs slightly younger than the Sun. The systematic pattern of O, Mg, Si, and Fe coronal abundances generally found for solar-type stars observed with ASCA is puzzling, because it does not appear related either to the photospheric composition or to the activity level.

Key words: stars: coronae – stars: late-type – stars: abundances – stars: activity – X-rays: stars – stars: individual: 30 Ari – stars: individual: η Boo

1. Introduction

The metal abundance of the emitting plasma is one of the parameters which is expected to have an influence on the structure of the corona in late-type stars. In fact, the spectrum of a plasma at the typical temperatures observed in solar-like stellar coronae (few million K) is dominated by line emission, hence metallicity may affect the emissivity of the plasma and thus its radiative losses. Also, the relative contribution of line and continuum emission varies with temperature, and therefore the variation of radiative losses with temperature will also be metallicity-dependent. As a consequence, all other parameters being the same, two identical stars with different metal abundance might show significantly different coronae.

To ascertain the influence of metal abundance on coronal characteristics it is thus of interest to study stars spanning a range of metallicities as large as possible. Up to now, however, most coronal sources studied at sufficient spectral resolution (i.e. with the ASCA satellite) span a rather small range of metal abundances, with most sources having derived coronal metal abundances below the solar value (Jordan et al. 1998). It remains unclear whether this is due to the photospheric abundances of the sources being lower than solar or to the coronal abundances of the observed stars being depleted relative to the photospheric ones. The fact that many well-studied, active coronal sources do not have well-determined photospheric abundances may also contribute to the problem. Whatever the reason for the small observed range of coronal metallicities, in practice this means that only a small fraction of the abundance values observed in stellar photospheres has been studied in stellar coronae: typical best-fit coronal metal abundance values reported in the literature for active stars observed with ASCA range from $\simeq 0.5$ down to $\simeq 0.2$ times the solar value. The only exceptions known so far are the few field G-type dwarfs for which ASCA X-ray spectra have been obtained (Güdel et al. 1997; Mewe et al. 1998): they show coronal iron abundances near or slightly below the solar (photospheric) value, but systematically higher $\rm Mg/Fe$ and $\rm Si/Fe$ abundance ratios, and systematically lower $\rm O/Fe$ ratios. Most recently, also the active binary Capella has been found to be an exception by Brickhouse et al. (1999), who have performed a detailed analysis of simultaneous ASCA and EUVE spectra (see Sect. 4.1 for some detail), and found solar abundances for all the elements, except Ne.

Send offprint requests to: amaggio@oapa.astropa.unipa.it

We have therefore started a program aimed at observing the coronal emission of stars with well-determined photospheric abundances, and in particular of sources classified as "Super Metal-Rich" (SMR). In the present context, we have adhered to a definition of super metal-richness based on the criterion [Fe/H]≥ 0.2 (where the square brackets are used to indicate the logarithm of the value in solar units). The aim of the program was twofold: on one hand, by studying stars with well-determined photospheric abundances (based on modern high-resolution spectroscopic studies) we can compare the photospheric and coronal metal abundance on a firmer ground. At the same time, we expect that the coronal abundance would turn out to be higher than what has been observed in many coronal sources until now, thus allowing for the study of a truly metal-rich corona.

2. Target selection

We have started our source selection process by taking as candidates the bright F, G and K stars whose photospheric abundances have been determined through high-resolution spectroscopy, using the extensive compilation of data of Taylor (1994; 1996), who has critically examined the spectroscopic abundance determinations available in the literature and reduced them to a single effective temperature scale. All sources with $[\mathrm{Fe/H}]$ higher than 0.2 have been considered as possible candidates. The ROSAT All Sky Survey Bright Source Catalog (RASS-BSC) and the various available ROSAT catalogs of X-ray sources have been searched for X-ray flux data, retaining as candidates those stars which, based on an average flux to count rate conversion factor (assuming a spectrum "typical" of coronal sources), would produce a sufficiently high count-rate in the ASCA-SIS detector for X-ray spectroscopy to be performed. This process resulted in five possible candidates, of which two have been observed, as part of the present program, during the ASCA AO5 cycle, i.e. HR 5235 (HD 121370) and HR 764 (HD 16232).

HR 764 (30 Ari B) is an F4 dwarf, of apparent magnitude 7.1. with a bright ($V = 6.5$) companion (HR 765, F6 III) at 42 arcsec separation, with which it likely forms a physical pair. The photospheric metallicity of HR 764, $[\mathrm{Fe/H}] = 0.250$ (Taylor 1996), is about twice the solar value. This star has been detected in the ROSAT All Sky Survey (RASS) with a count rate of 0.47 cts s^{-1}, as reported by Huensch et al. (1998), but it is not present in any pointed *Einstein* Observatory or ROSAT/PSPC observation, so that our ASCA data provide the first X-ray spectrum of this star.

HR 5235, better known as η Boo, is a well-studied bright ($V = 2.7$), nearby sub-giant, with a Hipparcos parallax $\pi = 88.17 \pm 0.75$ mas and spectral type G0 IV. Its metallicity, at $[\mathrm{Fe/H}] = 0.305$ (Taylor 1996), appears slightly higher than for HR 764, but it is also significantly fainter in X-rays. It is present in the RASS-BSC, as well as in three serendipitous PSPC observations, with an X-ray count rate of about 0.1–0.2 cts s^{-1}, in the 0.1–2.4 keV band. It has a fainter ($V = 8.8$) optical companion at 113 arcsec separation, which however does not show significant X-ray emission in the ROSAT PSPC pointed observations, and is therefore not expected to contaminate the ASCA data. The spectral analysis of one of the PSPC data sets has been recently performed by Ventura et al. (1998), adopting both two-component isothermal models and detailed coronal loop models, with the assumption of a plasma with solar abundances; their results will be recalled in Sect. 5, and discussed in the light of our new ASCA data.

We note in advance that the observed targets are relatively X-ray faint, compared with the very active and/or nearby stars which have been the subject of most ASCA spectral studies so far. However, they are the best targets – in our knowledge – which allow study of the X-ray emission of SMR coronal sources.

3. The ASCA observations

The ASCA observation of η Boo was performed between Dec. 28, 1996, and Jan. 4, 1997, while 30 Ari was observed on Aug. 24–25, 1997. In both cases the data were acquired with the two Solid State Imaging Spectrometers (SIS0 and SIS1) in the 1-CCD mode, and with the two Gas Imaging Spectrometers (GIS2 and GIS3).

Due to the relatively low count rates of the sources, we have taken special care in the data reduction. We have considered both the data obtained with the standard REV2 processing, and new data sets obtained with optimized screening criteria, aiming at increasing the signal-to-noise ratio at the expense of a slight reduction in the total number of counts. In fact, we have found consistent spectral fitting results in the two cases, thus increasing the confidence in our conclusions. However, we were unable to solve some cross-calibration problems between the various detectors, especially for the more recent observation of HR 764, so that most of our conclusions are based on the analysis of the SIS0 data, which appear to be the most reliable.

The elongated shape of the photon cloud, clearly visible in the ASCA/SIS observation pointed toward HR 764 (Fig. 1), suggests that also its companion, HR 765, is an X-ray source, although significantly fainter. In fact, the approximate X-ray source positions (J2000 RA $2^h\ 37^m\ 2^s$, DEC $+24^d\ 39^m\ 1^s$, and RA $2^h\ 37^m\ 4^s$, DEC $+24^d\ 38^m\ 55^s$ of HR 764 and HR 765 respectively), are consistent with the optical positions at the epoch of the observation. Given the low spatial resolution of the instruments, we were unable to derive a more quantitative estimate of the relative fluxes, and the extracted spectra include the contributions of both stars.

The screening criteria applied to the SIS data exclude the first 2000 sec of the HR 764 observation, due to bad pointing accuracy. Other criteria, applied also in the case of HR 5235, were: elevation angle between Earth's limb and pointing direction (ELV) > 5 degrees, South Atlantic Anomaly flag (SAA) $= 0$, and Bright Earth Angle (BR_EARTH) ≥ 10 degrees. All the other criteria used in the standard REV2 processing, for instance Cut-off Rigidity (COR) > 6 GeV/c, were also investigated and found to be not relevant to our SIS data and/or analyses. Instead, for the GIS data, a criterion COR > 7 was also applied, and this implies an exposure time for the GIS shorter

Table 1. X-ray observation summary

			SIS0			GIS2		
Target Name	HR	Observation ID	Exposure ksec	Rate[a] cts s^{-1}	Frac[b] %	Exposure[c] ksec	Rate[a] cts s^{-1}	Frac[b] %
30 Ari	764	25042000	63.1	0.071	88.6	54.2	0.014	86.1
η Boo	5235	25041000	223.4	0.017	59.7	119.3	0.003	33.9

[a] Background-subtracted source count rates in the 0.5–3 keV band for the SIS spectra, and in the 0.6–2 keV band for the GIS spectra
[b] Fraction of the total (source + background) count rate
[c] Dead-time corrected

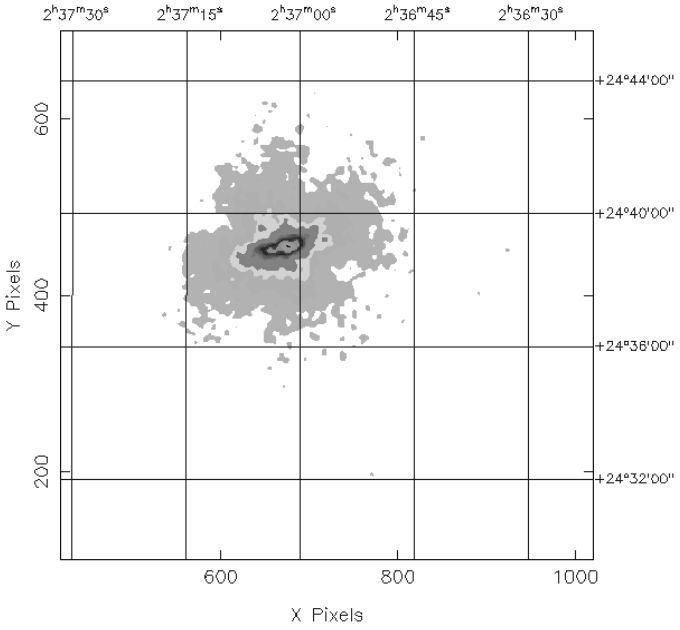

Fig. 1. ASCA/SIS image of HR 764 in the 0.5–2 keV band. Note the elongated shape of the source, due to the faint X-ray emission of the companion, HR 765. The two stars are at 42 arcsec separation.

than for the SIS. In the case of the observation of η Boo, the GIS exposure time is much shorter than the SIS one because the operations were suspended six times for technical reasons.

Such a screening resulted in useful exposure times of about 63 ksec and 220 ksec for 30 Ari and η Boo, respectively, reported in Table 1 together with the resulting count rates and other relevant information.

We have carefully checked the BR_EARTH screening criterion because low BR_EARTH values may yield a soft energy excess due to Solar X-rays scattered by the Earth atmosphere. Fortunately, satellite attitudes in our observations allowed us to use data with BR_EARTH ≥ 10: in fact, we have verified that the source spectra extracted with this criterion show no systematic discrepancy from spectra obtained with more restrictive criteria (e.g. BR_EARTH > 30), and that no increase of dark frame error (DFE) values occurs. Moreover, we have verified that no X-ray excess below 0.7 keV is visible even in SIS0 data selected with $10 \leq$ BR_EARTH < 15 (where scattered solar X-rays could be most evident), or in the background spectra. We conclude that the X-ray spectra of our targets are not contaminated by solar X-rays.

We have also investigated, in the case of the HR 764 observation, the Residual Dark Distribution (RDD) effects, due to radiation damage of the SIS CCD detectors. The correction, performed with the CORRECTRDD tool, yields less noisy SIS spectra, but it has not helped to solve the discrepancy between the SIS0 and SIS1 data, or the slight gain correction required to fit the SIS0 spectrum (see below).

We have accumulated the counts and the pulse height (PI) spectra from circular regions of about 3.5 arcmin radius for both the SIS and the GIS, thus ensuring a good compromise between S/N ratio and total number of counts. In the case of the two SIS images, we have also considered larger circular regions of 4.5 arcmin radius, removing the small sections which extend outside one of the edges of the CHIP1 CCD detector: this choice helped to reduce the statistical noise in the background-subtracted spectra, but the fitting results did not change significantly.

In the GIS images of η Boo, three more sources have been detected, and one more in the field of 30 Ari; these sources are fainter in X-rays than our targets, they fall at angular distances larger than 12 arcmin from our targets, and definitely outside the SIS fields of view, so they do not affect the extracted source spectra at all. They have been discarded from the GIS background region by removing circles of 6 arcmin radius centered on each of these serendipitous sources. The rest of the field of view, cleaned of all the detected sources, has been used to accumulate background spectra for each detector. The resulting background-subtracted count rates for our targets have been reported in Table 1.

The X-ray light curves of both sources do not show evidence of any large flaring event, but some low-amplitude variability, at the 25% level, was present during the observation of HR 5235: in fact, a simple statistical test again the hypothesis that the source was constant yielded a reduced χ^2 of 1.6 with 113 degrees of freedom, corresponding to a probability of $\sim 10^{-5}$.

The BRIGHT2 SIS spectra and the GIS spectra were rebinned to get at least 35 cts per bin, before background subtraction. We analyzed the SIS data in the spectral range 0.5–3 keV for HR 764, and in the range 0.5–2 keV for η Boo, because the spectral response below 0.5 keV is poorly known, and the source flux at energies higher than the chosen upper bound falls below the background level. For the GIS spectra, the low energy boundary

Table 2. 1-T model fitting results[a].

Star	$f_x/10^{-12}$ [b] erg/cm^2/s	T 10^6 K	$EM/10^{52}$ cm^{-3}	Abundances[c] O	Mg	Si	Fe	χ^2_r/dof[d]	Remarks
30 Ari	2.1	6.5 ± 0.2	1.3	= Fe[d]	$2.2^{+2.6}_{-0.9}$	$1.5^{+2.3}_{-0.6}$	$0.9^{+1.0}_{-0.3}$	1.1/59	O and Fe abundances linked
30 Ari	2.2	6.3 ± 0.3	1.8	$0.3^{+0.6}_{-0.2}$	$1.7^{+1.6}_{-0.7}$	$1.2^{+1.2}_{-0.6}$	$0.6^{+0.7}_{-0.2}$	1.0/58	
30 Ari	2.0	6.2 ± 0.3	1.2	$0.5^{+1.1}_{-0.4}$	$2.5^{+5.7}_{-1.2}$	$1.9^{+4.6}_{-1.0}$	$1.0^{+2.1}_{-0.4}$	0.9/57	High-n Fe line component included in the model
η Boo	0.8	3.6 ± 0.2	0.1	$0.2^{+0.1}_{-0.1}$	$1.4^{+3.1}_{-0.8}$	$2.0^{+5.0}_{-1.3}$	$0.4^{+0.8}_{-0.2}$	1.1/54	SIS0 and SIS1 joint fit

[a] The 90% confidence ranges have been computed with the criterion $\chi^2 < \chi^2_{min} + 2.7$ (Lampton et al. 1976).
[b] X-ray fluxes, corrected for the ISM absorption, in the 0.1–2.4 keV band.
[c] Abundances relative to solar system values: O = 8.93, Mg = 7.58, Si = 7.55, Fe = 7.67 (in logarithmic units, with H = 12.00).
[d] Reduced χ^2 and number of degrees of freedom

has been fixed at 0.7 keV, while high energy boundaries similar to the above ones have been defined.

For the extraction of the X-ray spectra we used XSELECT V1.3, and the utilities SISRMG V1.10 and ASCAARF V2.72 of the package FTOOLS V4.0 for creating appropriate instrument response matrices and auxiliary response files (ARFs).

For the spectral analysis we employed multi-component isothermal models, using the software package XSPEC V10.00 to perform a χ^2 fitting of the observed spectra and to compute statistical confidence regions in the model parameter space. In both cases we adopted the MEKAL emissivities for an optically-thin plasma in collisional equilibrium, computed by Mewe et al. (1985; 1986; 1995), based on the ionization balance of Arnaud & Raymond (1992) for iron. The reference element abundances of the coronal plasma are the solar system ones of Anders & Grevesse (1989), and all the abundance values derived with the spectral fitting are relative to these values: in particular, the assumed solar abundances of O, Mg, Si, and Fe are 8.93, 7.58, 7.55, 7.67, respectively (in a logarithmic scale where H=12.0). We note in passing that Grevesse et al. (1992) have recommended slightly lower values for O (8.87) and Fe (7.51).

4. Results

The results of the spectral fitting with isothermal models are summarized, for both stars, in Table 2. Similar procedures and tests have been applied in the two cases, but a detailed description will be presented in the following only for the case of 30 Ari, because of the better S/N ratio of the collected spectra. For conciseness, the section dedicated to η Boo is focused just on the final results of the analysis.

4.1. 30 Ari

The SIS0 spectrum to which the following results refer, is the one extracted from the RDD-corrected event file, using a source region of 3.5 arcmin radius (falling entirely within the CCD frame). Some comments on the results obtained with other choices are reported at the end of this section.

We first attempted to fit the SIS0 and GIS2 spectra with one- or two-component (1-T or 2-T) isothermal models, including the plasma metallicity, Z, as free parameter, i.e. keeping fixed all the element abundances relative to the solar values. In this, as in all other fits discussed later for this source, the interstellar column density, $N_{\rm H}$, was fixed at 1×10^{19} cm^{-2}, as estimated from its Hipparcos parallax ($\pi = 25.36 \pm 1.10$ mas) and an assumed mean interstellar hydrogen density of 0.07 cm^{-3} (Paresce 1984). Given the relatively hard bandpass of the SIS detector ($E \gtrsim 0.5$ keV), column densities of this order of magnitude have very little influence on the derived spectral parameters.

The 2-T best-fit model indicates the presence of a dominant component at $\sim 6 \times 10^6$ K, and a hotter component at $\sim 4 \times 10^7$ K, with a volume emission measure (EM) 18% the value found for the cooler component; the metallicity is about 0.7 solar. However, the fit quality is quite poor (reduced χ^2 = 1.4 with 85 d.o.f., corresponding to a probability level of 0.6%), due to large residuals especially evident at 1.3 keV and 1.8 keV, where the model under-predicts the strength of the He-like emission lines due to Mg XI and Si XIII. The presence of the hotter component, whose contribution is relevant only in the high-energy tail ($E > 2$ keV) of the spectrum, is driven by the need to increase the predicted number of counts near the Si XIII feature.

Therefore, we have subsequently fit the data with a 1-T model in which the Mg and Si abundances were left free to vary individually, while all the other element abundances were linked to the Fe abundance. The quality of the fit improves significantly (probability 62%), yielding Fe, Mg, and Si abundances of 0.9, 2.2, and 1.5, respectively, and a plasma temperature similar to the one of the cooler component in the 2-T fit above. Although this fit is now formally acceptable, there are systematic residuals between 0.6–0.7 keV (model excess), and in the region 1.1–1.3 keV (model defect). The former problem can be explained as an overprediction of the O VII and O VIII line intensities, expected to be strong for a plasma with solar abundances. In fact, the inclusion of the O abundance among the free parameters of the model, yields to a further slight improvement of the fit quality (Table 2), and to the following best-fit values: T = 6.4×10^6 K

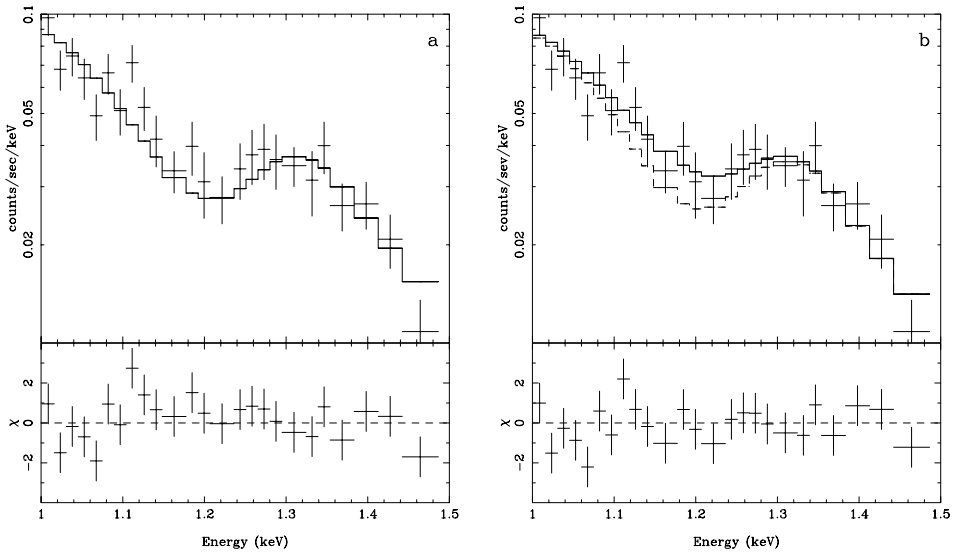

Fig. 2a and b. ASCA/SIS0 spectrum of 30 Ari, with best-fit models and residuals, χ (divided by the data errors), in the region around 1.2 keV. In **a** we show a pure 1-T MEKAL model with O, Mg, Si, and Fe variable abundances. Note the systematically positive residuals in the range 1.1–1.3 keV. In **b**, the fitting model (solid line) includes a 1-T component (dashed line) similar to the one above, and an additional gaussian component which accounts for Fe XVII line emission from highly excited states. Note how the inclusion of the latter component yields residuals more evenly distributed around zero than in **a**. The global χ^2 decreases from 56.8 to 52.0 (with 58 and 57 degrees of freedom, respectively).

(unchanged), O = 0.3, Mg = 1.7, Si = 1.2, Fe = 0.6. However, the systematic positive residuals between 1.1–1.3 keV do not disappear (Fig. 2a).

We have then investigated whether the latter residuals may be due to the lack of Fe L shell lines from high-energy levels in the MEKAL emissivity model (Brickhouse 1998; Brickhouse et al. 1999). In fact, Liedahl & Brickhouse (1999) show that, in the spectral range 1.14–1.46 keV, fall a large number of Fe XVII, Fe XVIII and Fe XIX emission lines which originate from atomic levels with high quantum numbers ($n > 5$). These ions reach their maximum concentrations in the temperature range 5–8 MK, hence the X-ray spectrum of 30 Ari, indicating an average coronal temperature of 6 MK, very likely includes these high-excitation lines. In order to test this hypothesis, we have fitted our X-ray data with a new model including – in addition to the isothermal MEKAL component adopted so far – a gaussian component with central energy, $E_{\rm g}$, left free to vary in the range 1.1–1.5 keV, line width $\sigma = 0.05$ keV, and intensity dynamically evaluated during the fit with the following expression:

$$I(T) = KA_{Fe}G(T) \qquad (1)$$

where $K = EM/(4\pi D^2)$ is the normalization of the isothermal component (with EM the plasma volume emission measure and D the star distance), A_{Fe} is the iron abundance relative to the solar value, which is also one of the free parameters of the MEKAL component, and $G(T)$ is the total emissivity due to Fe XVII–XIX lines, computed by Liedahl & Brickhouse (1999), as a function of plasma temperature, T. Note that the new model has just one free parameter[1] more than the 1-T model used before, namely $E_{\rm g}$. As a result of the addition of the gaussian component, with a best-fit value of the central energy $E_{\rm g} = 1.18$ keV and total intensity $I = 1.4 \times 10^{-5}$ photons cm^{-2} s^{-1}, the residuals around 1.2 keV are greatly reduced (Fig. 2). At the best-fit temperature of 6.2×10^6 K, most of the emission in the gaussian component is due to Fe XVII ions (67% of the total), and this is consistent with the value of $E_{\rm g}$ found near the low-energy boundary of the allowed range.

A further, not obvious effect is an increase of all the element abundances with respect to the case where the $\rm high - \it n$ Fe line contribution is ignored. In fact, the final best-fit values are the following: O = 0.5, Mg = 2.5, Si = 1.9, Fe = 1.0. A similar behavior of the abundances was noted by Brickhouse et al. (1999) while fitting the ASCA spectrum of Capella. A tentative explanation offered there is that, in absence of the high-excitation Fe XVII lines, the fitting algorithm artificially rises the continuum in order to minimize the residuals between 1.1–1.3 keV, and this implies lower line-to-continuum ratios and hence lower abundances.

Since Ne X has a very strong Lyα line at 1.02 keV, closely blended with other Fe XVII lines, and also a Lyβ line at 1.21 keV with emissivity comparable to those of the high-n Fe lines, we have checked whether allowing the Ne abundance to float has any influence on the spectral fitting results: the best-fit Ne abundance turns out to be $0.8^{+1.9}_{-0.6}$ solar, and the values of the other parameters do not vary significantly; in particular, the iron abundance is again 0.9 solar.

We conclude that the addition of the high-n Fe line component is appropriate in the case of 30 Ari since atomic physics suggests its presence, it is not included in the XSPEC thermal models, and it clearly improves the fit quality. On the other hand, the S/N ratio of the ASCA/SIS spectrum is such that – from a purely statistical point of view – this model refinement is not needed to get an acceptable χ^2. Best-fit results and related statistical uncertainties are reported in Table 2, while the observed spectrum and the final best-fit model are shown in Fig. 3.

[1] In order to reduce the number of free parameters, the line width, σ, has been fixed to a value about equal to the expected energy resolution of the SIS0 at 1 keV, at the time of the ASCA observation of 30 Ari (Dotani et al. 1997). If this parameter is left free to vary, its best-fit value converges to ~ 0.06 keV

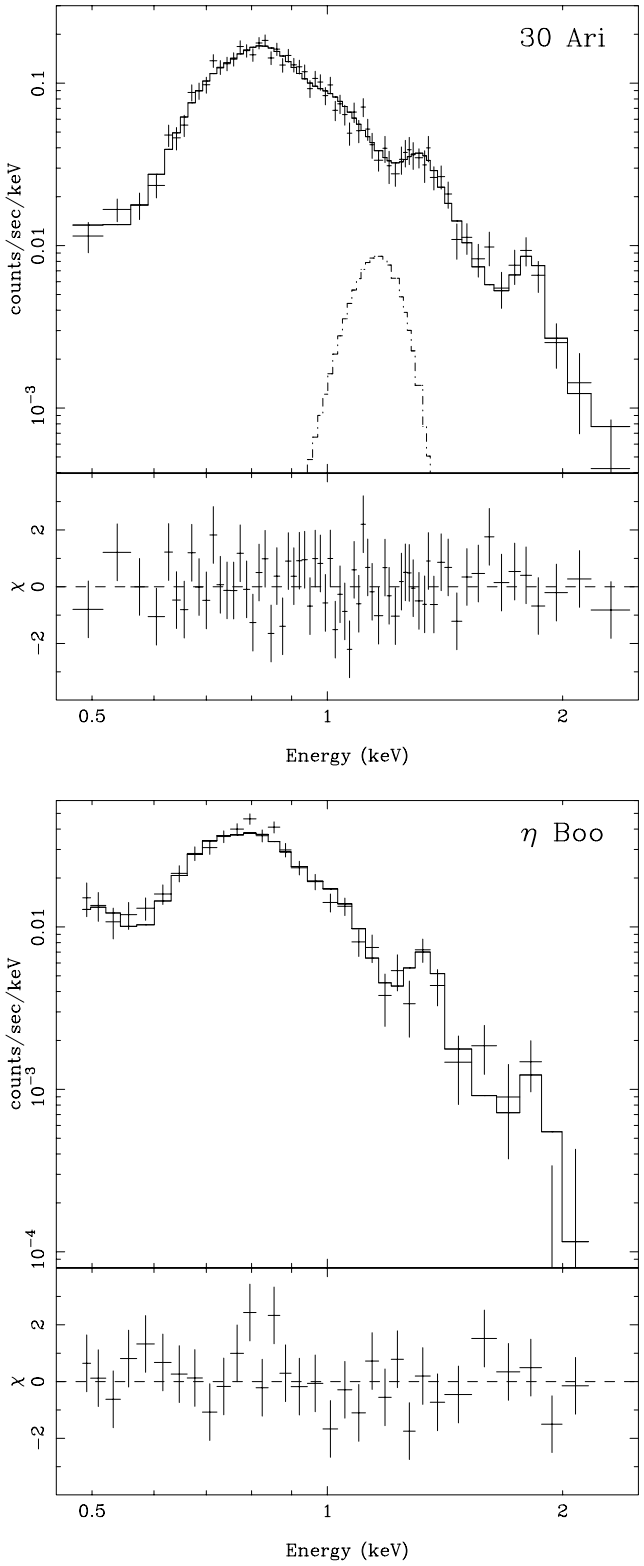

Fig. 3. ASCA/SIS0 spectra of 30 Ari and η Boo, and best-fit 1-T MEKAL models having O, Mg, Si, and Fe abundances as free parameters. In the top figure, the high-n Fe line gaussian component of the best-fit model is also shown (dashed line). Note the intense Mg XI and Si XIII emission lines near 1.3 keV and 1.8 keV, due to a relative overabundance of these two elements with respect to the iron abundance.

One of the reasons for the relatively large uncertainties on the element abundances is due to the correlation between the metallicity (mainly represented by the Fe abundance) and the plasma emission measure (i.e. the model normalization): in fact, due to its softness, most of the spectrum is dominated by the iron lines, with little contribution from the continuum, and this implies that a variation of the Fe abundance can be easily mimicked by a variation of the emission measure (Favata et al. 1997). As a consequence, the abundances relative to iron are better constrained than the ones relative to hydrogen (see also Mewe et al. 1998).

Following this argument, we have estimated the $\mathrm{O/Fe}$, $\mathrm{Mg/Fe}$, and $\mathrm{Si/Fe}$ abundance ratios and their uncertainties, by fixing the iron abundance to the extremes of the range found above, and computing the confidence limits on the abundances of the other elements, in each case. The $\mathrm{O/Fe}$, $\mathrm{Mg/Fe}$, and $\mathrm{Si/Fe}$ abundance ratios, reported in Table 3, indicate an O underabundance of about a factor 2, with respect to the solar $\mathrm{O/Fe}$ ratio, and relative overabundances of factors 2–3 for Mg and Si, in the corona of 30 Ari. If the Ne abundance is included among the free parameters, the resulting Ne/Fe ratio is $0.84^{+0.12}_{-0.07}$, i.e. consistent with the solar value; we note in passing that for Capella, the only other case in which the contribution from high-excitation Fe lines has been considered, the Ne/Fe ratio was found lower than solar by a factor ~ 3.

We have checked the robustness of the above results by fitting spectra extracted with different criteria. In particular, we have considered the spectra extracted from the event file generated with the standard REV2 data reduction and screening, spectra with and without correction for Residual Dark Distribution (RDD) applied, and spectra extracted from a larger source region, as already anticipated in Sect. 3. The fitting results are consistent in all cases, within the statistical uncertainties. The only effect worth noting, is that if no RDD correction is applied to the data the gain slope (energy to PI channel relation) needs to be decreased by about 3% from the nominal value, in order to fit properly the prominent Mg and Si emission features near 1.3 and 1.8 keV; with the RDD correction applied, a decrease of the gain slope of 1% only is sufficient to get the best-fit. On the other hand, in all of the above attempts, we were unable to get acceptable fitting results if the SIS1 spectrum is included in the analysis, and in fact, even the SIS1 spectrum alone cannot be fitted satisfactorily, while the SIS0 and GIS2 data appear consistent with each other.

Finally, we report that the spectral fitting yields a source flux of 2×10^{-12} erg cm^{-2} s^{-1}, in the energy band 0.1–2.4 keV (here employed for ease of comparison with ROSAT fluxes), which implies a source X-ray luminosity $L_{\mathrm{x}} = 4 \times 10^{29}$ erg s^{-1}.

4.2. η Boo

Due to the low X-ray flux of this source and its softness, the resultant GIS spectra are too noisy to attempt any reliable spectral fitting, so we have focused our attention on the SIS0 and SIS1 spectra. Since individual analyses of these spectra yield

Table 3. Abundance ratios[a]

Star Name	O/Fe	Mg/Fe	Si/Fe	Fe	$(Fe/H)_{phot}$	Ref.[b]
30 Ari	$0.6^{+0.2}_{-0.3}$	$2.6^{+0.1}_{-0.2}$	$2.0^{+0.1}_{-0.1}$	$1.0^{+2.1}_{-0.4}$	1.8	1
η Boo	$0.6^{+0.2}_{-0.2}$	$3.4^{+0.3}_{-0.4}$	$5.1^{+0.5}_{-0.6}$	$0.4^{+0.8}_{-0.2}$	2.0	1
α Cen	0.4±0.1	4.4±1.0	5.8±4.2	$0.77^{+0.37}_{-0.23}$	1.3–2.0	2
EK Dra		2.3		$0.99^{+0.30}_{-0.20}$		3
HN Peg		2.1		$0.72^{+0.40}_{-0.35}$		3
κ^1 Cet		2.3		$0.98^{+0.37}_{-0.23}$	0.9±0.1	3
π^1 UMa[c]	0.6	2.8	1.1	$0.41^{+0.24}_{-0.10}$	0.9±0.1	4

[a] Relative to solar values
[b] References: (1) this work, (2) Mewe et al. (1998), (3) Güdel et al. (1997), (4) Drake et al. (1994)
[c] Analysis of ASCA data performed with the MEKA thermal model; the improved MEKAL model was used in the other cases.

compatible results, we proceed to describe the results of the fits performed jointly on the two SIS data sets.

For this star we have neglected the interstellar absorption, because of the low hydrogen column density, $N_{\rm H} = 2 \times 10^{18}$ cm^{-2}, determined from the ROSAT data (Ventura et al. 1998), fully compatible with the very small distance to η Boo (11.3 pc).

Also for this target a 1-T model provides an acceptable fit of the data, but only if the Mg and Si abundances are left free to vary, independently of the abundances of iron and of the remaining elements in the model (C, N, O, Ne, Na, Al, S, Ar, Ca, and Ni) all linked together. Systematic residuals (model excess) near 0.6 keV suggest, as in the case of 30 Ari, that the O abundance could be also included among the free parameters, and this choice yields an improved fit quality. Instead, no contribution from high-n Fe XVII–XIX lines is required: in fact, such a contribution is negligible at the relatively lower coronal temperature of η Boo (see below).

The final best-fit model yields a reduced χ^2 of 1.1 with 54 d.o.f., and the following parameter values (see Table 2): $T = 3.6 \times 10^6$ K, O = 0.2, Mg = 1.4, Si = 2.0, Fe = 0.4, with the relatively large uncertainties reported in Table 2. While these individual abundances do not provide a clear constraint on the plasma metallicity, the abundance ratios with respect to Fe appear well determined: for example, if we keep the Fe abundance fixed to the photospheric value reported by Taylor (1996), i.e. Fe = 2 (five times the best-fit value), the other abundances all increase by about a factor 5, so that their ratios with respect to Fe remain fairly unchanged (see best-fit values and uncertainties reported in Table 3). The plasma temperature is also little affected, while the normalization (i.e. the plasma emission measure) decreases by about the same factor of 5, in order to match the overall source flux, which is 8×10^{-13} erg cm^{-2} s^{-1}, in the 0.1–2.4 keV band. The latter result implies an X-ray luminosity of 1.2×10^{28} erg s^{-1}, for the corona of η Boo.

5. Discussion

The two targets presented in this paper share the following property: they are both relatively soft and X-ray faint, when compared to the several active coronal sources observed with ASCA so far. This should not come as a big surprise for three key reasons: (i) super-metal-richness is a rare phenomenon, so that very few members of this class are within the spectroscopic capabilities of present-day instruments; this gives very little freedom in the choice of the targets; (ii) the active coronal sources, usually belonging to the class of the RS CVn binaries, are also exceptional sources, when compared to solar standards; while this makes the observations easier, the interpretation of their coronal X-ray emission may not be appropriate under the solar paradigm, so that a comparison with "normal" solar-type stars is usually difficult; (iii) one of the aims of our observation program was, in fact, to observe X-ray sources with characteristics different from those of the active stars which have attracted, for obvious reasons, the attention of most studies so far.

We recall that 30 Ari has been already observed in X-rays only once in the past, during the ROSAT All-Sky Survey. The PSPC count rate reported by Huensch et al. (1998) is a factor 1.6 higher than predicted by the model best-fitting the ASCA spectra. This difference may be due to source variability or to the presence of coronal plasma at temperatures of few million degrees, not detectable with ASCA because of the harder spectral band with respect to ROSAT. η Boo instead, has been observed both with the *Einstein* Observatory (Maggio et al. 1987) and four times with ROSAT, before the present ASCA pointing: taking into account the different bandpasses of the three instruments, the X-ray fluxes show a scatter of less than 20%. In particular, an acceptable fit of the ROSAT/PSPC spectrum (Ventura et al. 1998), was achieved with a 2-T model having $T_1 = 1.6 \times 10^6$ K, and $T_2 = 5.0 \times 10^6$ K, with a ratio of the emission measures $EM_1/EM_2 = 2.4$. A good description was also obtained with a more physically detailed coronal loop model, with plasma maximum temperature $T_{\rm max} = 3.5 \times 10^6$ K, and plasma pressure, $p_0 = 1$ dyn cm^{-2}, almost constant along loops having semi-length smaller than the pressure scale height

($H_p \sim 8 \times 10^{10}$ cm), and covering less than 20% of the stellar surface. The X-ray luminosity[2], at the time of the ROSAT observation in 1992, was estimated to be 1.3×10^{28} erg s^{-1}, and the same value was measured at the time of the ROSAT All Sky Survey observation in 1990 (Schmitt 1997). Given the low spectral resolution of the PSPC, the above results are little affected by the actual value of the plasma metallicity, which we have now estimated to be about half the value assumed in the previous works. We conclude that η Boo is indeed a low-activity coronal source, having similar X-ray luminosities measured in the 20 year time span between the *Einstein* and the ASCA observations, and little variations of the coronal temperature, as well.

In order to ascertain whether the coronae of the super-metal-rich stars 30 Ari B and η Boo are similar to those of other "normal" stellar X-ray sources, we start by comparing their plasma temperatures and X-ray luminosities with those derived for stars of similar spectral type in recent X-ray surveys.

From the first studies based on *Einstein* data (Schmitt et al. 1985; Maggio et al. 1987) and on the ROSAT All Sky Survey (Schmitt 1997), we know that the X-ray luminosity function of the F dwarfs in the solar neighborhood spans about two orders of magnitude, with a median $L_{\rm x} \sim 10^{28}$ erg s^{-1}, while the "normal" G dwarfs are slightly less luminous on average (median $L_{\rm x} \sim 2 \times 10^{27}$ erg s^{-1}), but they span almost three decades in X-ray luminosity. The large spread in X-ray luminosities is nicely interpreted as an effect of stellar aging, with the consequent spin down of the stellar rotation rate and a less efficient magnetic dynamo to power the stellar coronae. The correlated decay of X-ray luminosity, rotation, and mean coronal temperature with age has been recently revisited by Güdel et al. (1997), based on a selected sample of solar-type stars observed with ROSAT and ASCA. The coronal characteristics of η Boo fit nicely into this picture: in fact, its X-ray luminosity and coronal temperature are typical of other G-type dwarfs of age about half the solar one (2–3 Gyr), like β Com or 15 Sge. An age of 2.3 Gyr has been estimated by Guenther & Demarque (1996) for η Boo, based on comparison of observed p-mode frequencies with model predictions.[3]

30 Ari B, classified as a member of the Hyades moving group by Eggen (1982), shows a higher coronal luminosity ($\log L_{\rm x} = 29.3$ erg s^{-1}, assuming that $1/3$ of the measured value is due to its companion, HR 765) which can be favorably compared with the emission level of the X-ray bright F dwarfs in the Hyades cluster studied by Stern et al. (1995). On the other hand, its coronal temperature is also surprisingly similar to that measured in early-G dwarfs of the same age and X-ray luminosity, like BE Cet (Güdel et al. 1997). The above analysis leads to the conclusion that the coronal properties of 30 Ari B and η Boo are typical of field F and G late-type stars of comparable age, which do *not* share the property of being super-metal-rich.

Coming to the issue of the coronal abundances, the available data suggest that the plasma metallicity is near solar or slightly below solar, but the large uncertainties do not allow us to prove whether or not the coronal metallicities are really different from the photospheric ones. Instead, the Mg and Si abundance ratios relative to the Fe abundance are systematically larger by factors 2–6 than in the solar system, while the O/Fe abundance ratios appear systematically smaller by about a factor 2. These abundance "anomalies" could be easily interpreted as a selective enhancement in corona of some metals, and a depletion of others, in a way similar to what is called the First Ionization Potential (FIP) effect in the solar corona[4] (Meyer 1985; Feldman & Widing 1990). Evidence for such an effect has been recently presented by Drake et al. (1997) also for α Cen, a solar-like low-activity star.

Unfortunately, there are several other pieces of evidence that cast doubts on this interpretation:

1. Iron itself is a low-FIP element (ionization potential $<$ 10 eV), which shares with Mg, Al, Si, and Ca the same overabundance of a factor 3–4 in the active regions of the solar corona (Laming et al. 1995), and factors 2–3, relative to high-FIP elements (O, Ne, S), in the corona of α Cen, according to the EUV line emission analysis of Drake et al. (1997). However, the iron abundance derived from the analysis of the ASCA X-ray spectra of α Cen (Mewe et al. 1998) was $0.8^{+0.4}_{-0.2}$ the solar value, i.e. slightly below the photospheric metallicity (Table 3). We have found similar behavior in the case of 30 Ari and η Boo, although our uncertainties are such that values consistent with the photospheric ones cannot be excluded. On the other hand, we can exclude that the coronal metallicity of 30 Ari, as measurable from its ASCA spectra, could be 3 times its photospheric abundance or more (at the 99% statistical confidence level), as expected if a solar-like FIP effect would exist. With the same confidence, we can also exclude metallicity values below 0.3 solar.
2. High Mg/Fe abundance ratios have been derived by Güdel et al. (1997) from the analysis of ASCA spectra of three G-type stars, EK Dra, HN Peg and κ^1 Cet (Table 3), while the Fe abundances are near solar (EK Dra, κ^1 Cet) or sightly subsolar (HN Peg); the early analysis of the ASCA PV phase observation of another young G-type star, π^1 UMa, reported by Drake et al. (1994), also yielded Mg/Fe = 2.7, and Fe = 0.4 solar; accurate photospheric metal abundances have been recently determined for two of the above stars (κ^1 Cet and π^1 UMa) by Ottmann et al. (1998), who reported [Fe/H] and [Mg/H] values which indicate Mg/Fe ratios 0.8–0.9.

[2] All the reported luminosities have been computed using the new Hipparcos parallax of η Boo, $\pi = 88.17$ mas

[3] We note in passing that their *predicted* stellar parallax would be more in agreement with the recent Hipparcos measurement if the Taylor (1996) metallicity [Fe/H]= 0.25 is used, instead of the value [Fe/H]= 0.19 they have adopted. In any case, this correction does not affect significantly the predicted stellar age.

[4] Here we adhere to the interpretation of the FIP effect as due to an enhancement of low-FIP elemental abundances in corona, rather than a depletion of high-FIP elements

3. Systematically low O abundances (0.3–0.4 solar) have been found for α Cen, π^1 UMa, our super-metal-rich stars, the active single giant β Cet (Maggio et al. 1998), and most active binaries observed by ASCA; very low N abundances, often consistent with zero, have been also derived in early analyses of ASCA data, before realizing that severe calibration problems affect the instrument response of the SIS below 0.5 keV (Dotani et al. 1996).

In conclusion, the element abundances found for our targets appear quite similar to those reported for other field late-type stars having different photospheric compositions and different X-ray emission levels, but we suspect that this puzzling result may be an artifact of the analysis.

The above arguments suggest that the common O, Mg, Si, Fe abundance patterns, obtained from the analysis of many ASCA data sets, may need careful re-examination in order to spot possible residual problems in the instrument calibration. In fact, since the abundances of most elements, excluding Fe, rely on the measure (implicitly performed by the fitting algorithm) of a single strong emission feature in the X-ray spectrum, such abundances are prone to systematic uncertainties due to calibration problems or even to the inadequacy of the assumed model spectrum to describe the "true" plasma emission measure distribution. The case of the iron abundance is different: since the bulk of the Fe emission lines fall near 1 keV, where the effective area of most of the currently available and upcoming instruments is higher, and since the plasma emissivity codes are likely missing many low-intensity lines in the same energy range (Brickhouse 1998; Wargelin et al. 1998), the results of spectral analysis based on parametric model fitting (rather than on line to continuum or line to line ratios) may yield biased Fe abundance values.

The issue of the coronal abundances is already in the agenda of the new X-ray spectroscopic missions Chandra, ASTRO-E and XMM, that will be launched in the next two years. The increased sensitivity of the new instruments will certainly allow us to address most of the questions above, and will give also the opportunity to make a new start of coronal physics through X-ray spectroscopy of the many low-active stars near the Sun.

Acknowledgements. AM acknowledges partial support from Ministero dell'Universitá e della Ricerca Scientifica e Tecnologica, and Agenzia Spaziale Italiana. AM also wishes to thank the collegues Dr. S. Sciortino and F. Reale for useful comments and suggesions. NB acknowledges support from the Chandra X-ray Observatory Center and NASA grant NAG5-3559. This work was also supported in part by grant NAG5-3389 from NASA to the Smithsonian Astrophysical Observatory.

References

Anders E., Grevesse N., 1989, Geochimica and Cosmochimica Acta 53, 157
Arnaud M., Raymond J., 1992, ApJ 398, 394
Brickhouse N.S., 1998, In: Donahue R.A., Bookbinder J. (eds.) Cool Stars, Stellar Systems, and the Sun. Tenth Cambridge Workshop, Vol. 154 of ASP Conf. Series, p. 487
Brickhouse N.S., Dupree A.K., Edgar R.J., et al., 1999, ApJ submitted
Dotani T., Mitsuda, K., Yamashita A., et al., 1996, AscaNews 4
Dotani T., Yamashita A., Ezuka H., et al., 1997, AscaNews 5
Drake J.J., Laming J.M., Widing K.G., 1997, ApJ in press
Drake S.A., Singh K.P., White N.E., Simon T., 1994, ApJ 436, L87
Eggen O., 1982, ApJS 50, 221
Favata F., Maggio A., Peres G., Sciortino S., 1997, A&A 326, 1013
Feldman U., Widing K.G., 1990, ApJ 363, 292
Grevesse N., Noels A., Sauval A.J., 1992, In: Coronal Streamers, Coronal Loops, and Coronal and Solar Wind Composition. pp 305–308
Güdel M., Guinan E.F., Skinner L.S., 1997, A&A 483, 947
Guenther D.B., Demarque P., 1996, ApJ 456, 798
Huensch M., Schmitt J.H.M.M., Voges W., 1998, A&AS 132, 155
Jordan C., Doschek G.A., Drake J.J., Galvin A.B., Raymond J.C., 1998, In: Donahue R.A., Bookbinder J. (eds.) Cool Stars, Stellar Systems, and the Sun. Tenth Cambridge Workshop, Vol. 154 of ASP Conf. Series, p. 91
Laming J.M., Drake J.J., Widing K.G., 1995, ApJ 443, 416
Lampton M., Margon B., Bowyer S., 1976, ApJ 208, 177
Liedahl D.A., Brickhouse N.S., 1999, ApJ submitted
Maggio A., Sciortino S., Vaiana G.S., et al., 1987, ApJ 315, 687
Maggio A., Favata F., Peres G., Sciortino S., 1998, A&A 330, 139
Mewe R., Gronenschild E., van den Oord G., 1985, A&AS 62, 197
Mewe R., Lemen J., van den Oord G., 1986, A&AS 65, 511
Mewe R., Kaastra J.S., Liedahl D.A., 1995, Legacy 6, 16
Mewe R., Drake S.A., Kaastra J.S., et al., 1998, A&A 339, 545
Meyer J.-P., 1985, ApJS 57, 173
Ottmann R., Pfeiffer M.J., Gehren T., 1998, A&A 338, 661
Paresce F., 1984, AJ 89, 1022
Schmitt J.H.M.M., 1997, A&A 318, 215
Schmitt J.H.M.M., Golub L., Harnden Jr. F.R., et al., 1985, ApJ 290, 307
Stern R.A., Schmitt J.H.M.M., Kahabka P.T., 1995, ApJ 448, 683
Taylor B.J., 1994, PASP 106, 704
Taylor B.J., 1996, ApJS 102, 105
Ventura R., Maggio A., Peres G., 1998, A&A 334, 139
Wargelin B.J., Beiersdorfer P., Liedahl D.A., Kahn S.M., Von Goeler S., 1998, ApJ 496, 1031